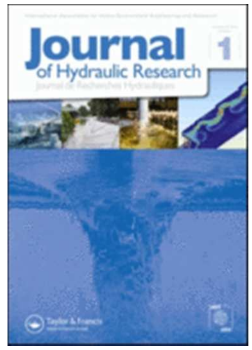

Computing flooding of crossroads with obstacles using a 2D numerical model

Journal:	*Journal of Hydraulic Research*
Manuscript ID	TJHR-2017-0024
Manuscript Type:	Discussion
Date Submitted by the Author:	27-Jan-2017
Complete List of Authors:	Bruwier, Martin; University of Liege (ULG), Hydraulics in environmental and civil engineering (HECE) Erpicum, Sébastien; University of Liège, ArGEnCo Archambeau, Pierre; University of Liège, ArGEnCo Pirotton, Michel; University of Liège, ArGEnCo Dewals, Benjamin; University of Liege, Urban & Environmental Engineering
Keywords:	
JHR Keywords:	

Discussion

Computing flooding of crossroads with obstacles using a 2D numerical model

By P.-H. BAZIN, E. MIGNOT and A. PAQUIER, *J. Hydraulic Res.* 54(6), 2016, 1-13

Discussers:

MARTIN BRUWIER, PhD Student, *Hydraulics in Environmental and Civil Engineering (HECE), Research unit Urban & Environmental Engineering, University of Liege, Liege, Belgium*

Email: mbruwier@ulg.ac.be (author for correspondence)

SEBASTIEN ERPICUM (IAHR Member), Research Associate, *Hydraulics in Environmental and Civil Engineering (HECE), Research unit Urban & Environmental Engineering, University of Liege, Liege, Belgium*

Email: s.erpicum@ulg.ac.be

PIERRE ARCHAMBEAU, Research Associate, *Hydraulics in Environmental and Civil Engineering (HECE), Research unit Urban & Environmental Engineering, University of Liege, Liege, Belgium*

Email: pierre.archambeau@ulg.ac.be

MICHEL PIROTTON, Full Professor, *Hydraulics in Environmental and Civil Engineering (HECE), Research unit Urban & Environmental Engineering, University of Liege, Liege, Belgium*

Email: Michel.pirotton@ulg.ac.be

BENJAMIN DEWALS (IAHR Member), Associate Professor, *Hydraulics in Environmental and Civil Engineering (HECE), Research unit Urban & Environmental Engineering, University of Liege, Liege, Belgium*

Email: b.dewals@ulg.ac.be

Discussion

Computing flooding of crossroads with obstacles using a 2D numerical model

Based on an operational 2D shallow-water model, the Authors computed subcritical dividing flow at a three-branch crossroad, considering obstacles located at different positions. The numerical predictions were compared to observations from Mignot et al. (2013). Two issues are addressed here, related respectively to the efficiency and relevance of the turbulence model, and to the representation of the obstacles in operational flood models.

1. Turbulence model

The Authors tested a single turbulence model, which is based on a constant eddy viscosity and leads to "acceptable results" after calibration. They argue that a more elaborate turbulence model is "not affordable for large-scale flood studies" due to an additional computational effort. Here, the Discussers show that a k-ε turbulence model competes with a simple turbulence model in terms of overall computational efficiency as the former requires no calibration.

For the case without obstacle, the Discussers simulated the 14 flow configurations considered by the Authors (Table 1 in Bazin et al., 2016) without turbulence model and with a k-ε turbulence model. The academic code Wolf2D was used with a coarse Cartesian grid of 5 cm × 5 cm (e.g., Arrault et al., 2016), leading to a similar accuracy on the discharge partition as in Bazin et al. (2016). Running the code with the k-ε turbulence model was about 1.6 times more demanding in terms of computational cost than one simulation without turbulence model. However, since the simple turbulence model used by the Authors requires at least two runs for calibrating the constant eddy viscosity coefficient K and/or for assessing the sensitivity of the results to the value of K, the overall computational burden of the k-ε turbulence remains lower than the use of the simple turbulence model.

As shown in Figure 1 and in Supplement 1, the values of the eddy viscosity computed by the k-ε turbulence model agree in average with the values tested by the Authors (between 0 and 10^{-3} m^2/s); but they vary substantially in space and from one flow configuration to the other. This challenges the operational validity of a constant eddy viscosity model since flood models are generally calibrated based on observed flood data, while they are subsequently used for more extreme flood scenarios.

Although the turbulence model does not alter significantly the computed discharge partitions, it provides more realistic velocity fields. This of practical importance in flood risk management, for instance for assessing hydraulic loads on obstacles and their stability. This finding, also reported by the Authors, is consistent with another recent flood study in a more complex urban setting involving a total of 49 crossroads (Arrault et al., 2016). Indeed, based on the k-ε turbulence model and a Cartesian grid, Arrault et al. (2016) showed that activating the turbulence model does not alter the discharge distribution in-between the 14 different streets of their setup, by more than 2 % compared to a computation without turbulence model. Slightly higher variations were found at some crossroads within the urban district, as a result of changes in flow structures such as control sections (e.g., Fig. 11 in Arrault et al. 2016). In contrast, as highlighted by the Authors (Fig. 3 in the original paper), the computed recirculation lengths were affected considerably by the turbulence model (Fig. 10 in Arrault et al., 2016).

2. Porosity-based model with a Cartesian grid

As stated in their Introduction, the Authors aim "to identify which meshing strategy (method for including obstacles …) is required" to estimate the large-scale effects of obstacles on the flow. Three approaches can be considered to account for obstacles at a large scale (Schubert and Sanders, 2012; Dottori et al., 2013): *(i)* increasing the roughness parameter, *(ii)* representing the obstacles as holes in the mesh or *(iii)* using a porosity-based model. The Authors analysed only the second one. The first one is indeed particularly crude; but Schubert et al. (2012) showed that the porosity-based model leads to the best balance between accuracy and run-time efficiency. Therefore, this third option must also be considered to come up with a more general conclusion. Here, the Discussers compare the results obtained by the Authors based on a standard shallow-water model and a non-uniform mesh (Run A of Bazin et al., 2016) with the predictions of a porosity-based shallow-water model applied on a relatively coarse Cartesian grid.

2.1. Numerical model

The shallow-water model with anisotropic porosity used here is the same as described in Sect. 5.2 of Arrault et al. (2016). It involves two types of porosity parameters: a *storage* porosity, defined at the centre of each cell, represents the void fraction in the cell; while a *conveyance* porosity, defined at the edges of the computational cells, reproduces the blockage effect due to obstacles (Sanders et al., 2008; Chen et al., 2012; Özgen et al., 2016). To capture the presence of obstacles nearby the edges, the value of the conveyance porosity is set to the minimum fraction of free length parallel to the edge over half a cell on either sides of the edge. The momentum equations involve the same drag loss term as in the formulation of

Schubert and Sanders (2012). The drag coefficient c_D^0 is set to its standard value for 2D flow and square shape obstructions: $c_D^0 = 2$ (Munson et al., 2006).

2.2. Results

Tests without obstacles

To ensure that the models of Bazin et al. (2016) and Arrault et al. (2016) behave similarly when no porosity parameters are considered in the latter, we first compare their respective results for a configuration without obstacle (see Sect. 2.3 in the original paper). To evaluate the computed discharge partitions against the experimental observations, we use the same metrics as in the original paper: the relative bias $\delta\left(Q_{b0}^*\right)$ and the relative root mean square error $\sigma\left(Q_{b0}^*\right)$, both averaged over the 14 hydraulic conditions considered by the Authors. As shown in Table 1, both models lead to virtually the same relative bias $\delta\left(Q_{b0}^*\right)$, while the value of $\sigma\left(Q_{b0}^*\right)$ is higher for the model used in Arrault et al. (2016), which was applied here with an overall grid spacing slightly coarser (5 cm) than the non-uniform grid (3 - 5 cm) of Bazin et al. (2016). Moreover, as shown in Supplement 2, the difference in the value of $\sigma\left(Q_{b0}^*\right)$ is mostly related to the results of test series S2, while both models perform very similarly for test series S1 and S3. Finally, this difference in the models performance is deemed limited compared to the probable values of experimental uncertainties, which are not reported in Table 1 of the original paper.

Tests with obstacles

Next, we use the porosity-based shallow-water to simulate, on a coarse Cartesian grid, configurations with obstacles which cannot be properly represented by a direct discretization on the Cartesian grid. A total of 98 simulations have been conducted, corresponding to the 14 different hydraulic conditions and the 7 distinct locations of the obstacle presented by the Authors. Here also, the performance of the model is assessed based on the same metrics as introduced in Eqs. (9) to (13) of the original paper.

The errors $\delta\left(\Delta R_{q1-7}\right)$ and $\sigma\left(\Delta R_{q1-7}\right)$ on the discharge partition modification ΔR_{q1-7} obtained by the Discussers are relatively close to the values of the Authors, even if the relative bias $\delta\left(\Delta R_{q1-7}\right)$ has an opposite sign (Table 2). The absolute value of $\delta\left(Q_{b1-7}^*\right)$ is significantly lower with the model of Arrault et al. (2016), while the error $\sigma\left(Q_{b1-7}^*\right)$ is smaller for the model of Bazin et al. (2016). For most simulations, the Authors and Discussers obtain very similar discharge partitions (Fig. 2). As highlighted by the Authors, discrepancies mainly occur for high upstream Froude numbers and for obstacles located upstream of the crossroad.

Extra-simulations have been conducted with the porosity model to evaluate the sensitivity of the results to the value of the drag coefficient (Table 2). Two extreme values reported in literature (Kim et al., 2015) have been tested: $c_D^0 = 1$ and $c_D^0 = 3$. The errors $\sigma\left(\Delta R_{q1-7}\right)$ and $\sigma\left(Q^*_{b1-7}\right)$ are found minimum for the standard value of $c_D^0 = 2$, while the values of $\delta\left(\Delta R_{q1-7}\right)$ and $\delta\left(Q^*_{b1-7}\right)$ are hardly affected (Table 2). This reflects a good predictive capacity of the porosity-based model since it performs best based on standard value of the drag coefficient, without the need for a case-by-case calibration.

Figure 1 Change in the discharge partition due to the presence of the obstacle, as obtained from the experimental observations as well as from the numerical models of Bazin et al. (2016) and Arrault et al. (2016).

3. Conclusion

In terms of overall computational efficiency, we show that a k-ε turbulence model outperforms a constant eddy viscosity model, which requires calibration and/or sensitivity analysis for operational flood modelling. Moreover, the values of the eddy viscosity are found highly dependent on the flow configuration. The added value of a turbulence model stems from the improved prediction of the velocity field, which is of practical importance for assessing issues such as the stability of obstacles, the impact of floating debris or scour effects.

We compared the numerical results obtained by the Authors using a standard shallow-water model with a non-uniform mesh, to computations performed on a coarse Cartesian grid with a shallow-water model including anisotropic porosity parameters. We obtained a similar accuracy in the results with a slightly lower number of cells. In addition, the porosity-based approach is much more flexible to account for complex obstacle geometries. If the obstacles considered by the Authors were not aligned with the channel walls, the meshing technique they used would fail and a more complex unstructured mesh would be needed. In contrast, our approach based on porosity parameters can accommodate any obstacle shape with a reduced number of cells. Although the time step is a function of the value of the storage porosity, techniques exist to overcome stringent time step limitations (e.g., the merging technique applied by Causon et al. (2000, 2001) in combination with a cut-cell approach). Finally, the use of Cartesian grids is particularly appealing since they enable a straightforward overlay of the computational mesh with widely available gridded data, such as digital elevation models obtained from remote sensing techniques (Kim et al., 2014). This hints that porosity-based shallow-water models combined with Cartesian grids may be of high relevance for inundation mapping in practice.

Acknowledgements

The Authors gratefully acknowledge Prof. Emmanuel Mignot for sharing the experimental and numerical data of Bazin et al. (2016).

Funding

The research was funded through the ARC grant for Concerted Research Actions, financed by the Wallonia-Brussels Federation.

Supplemental data

Figures representing computed maps of eddy viscosity and the relative errors on the lateral discharge for simulations without obstacles can be accessed in the online version of the paper.

References

Arrault, A., Finaud-Guyot, P., Archambeau, P., Bruwier, M., Erpicum, S., Pirotton, M., Dewals, B. (2016). Hydrodynamics of long-duration urban floods: Experiments and numerical modelling. *Natural Hazards and Earth System Sciences* 16, 1413–1429.

Bazin, P.-H., Mignot, E., Paquier, A. (2016). Computing flooding of crossroads with obstacles using a 2D numerical model. *Journal of Hydraulic Research* 1–13.

Causon, D.M., Ingram, D.., Mingham, C.G., (2001). A Cartesian cut cell method for shallow water flows with moving boundaries. *Advances in Water Resources* 24, 899–911.

Causon, D.M., Ingram, D.M., Mingham, C.G., Yang, G., Pearson, R.V., (2000). Calculation of shallow water flows using a Cartesian cut cell approach. *Advances in Water Resources* 23, 545–562.

Chen, A.S., Evans, B., Djordjević, S., Savić, D.A. (2012). A coarse-grid approach to representing building blockage effects in 2D urban flood modelling. *Journal of Hydrology* 426–427, 1–16.

Dottori, F., Di Baldassarre, G., Todini, E., (2013). Detailed data is welcome, but with a pinch of salt: Accuracy, precision, and uncertainty in flood inundation modeling. *Water Resources Research* 49, 6079–6085.

Kim, B., Sanders, B.F., Famiglietti, J.S., Guinot, V. (2015). Urban flood modeling with porous shallow-water equations: A case study of model errors in the presence of anisotropic porosity. *Journal of Hydrology* 523, 680–692.

Kim, B., Sanders, B.F., Schubert, J.E., Famiglietti, J.S. (2014). Mesh type tradeoffs in 2D hydrodynamic modeling of flooding with a Godunov-based flow solver. *Advances in Water Resources* 68, 42–61.

Mignot, E., Zeng, C., Dominguez, G., Li, C.-W., Rivière, N., Bazin, P.-H. (2013). Impact of topographic obstacles on the discharge distribution in open-channel bifurcations. *Journal of Hydrology* 494, 10–19.

Munson, B.R., Young, D.F., Okiishi, T.H. (2006). *Fundamentals of Fluid Mechanics*, 5th ed. New York: John Wiley & Sons.

Özgen, I., Zhao, J., Liang, D., Hinkelmann, R. (2016). Urban flood modeling using shallow water equations with depth-dependent anisotropic porosity. *Journal of Hydrology* 541, 1165-1184

Sanders, B.F., Schubert, J.E., Gallegos, H.A. (2008). Integral formulation of shallow-water equations with anisotropic porosity for urban flood modeling. *Journal of Hydrology* 362, 19–38.

Schubert, J.E., Sanders, B.F. (2012). Building treatments for urban flood inundation models and implications for predictive skill and modeling efficiency. *Advances in Water Resources* 41, 49–64.

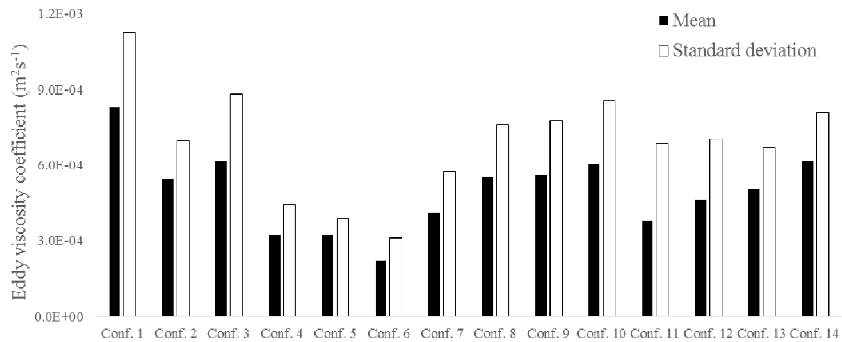

Figure 1 Mean value and standard deviation of the eddy viscosity computed with the *k*-*ε* turbulence model over the entire domain in the 14 flow configurations.

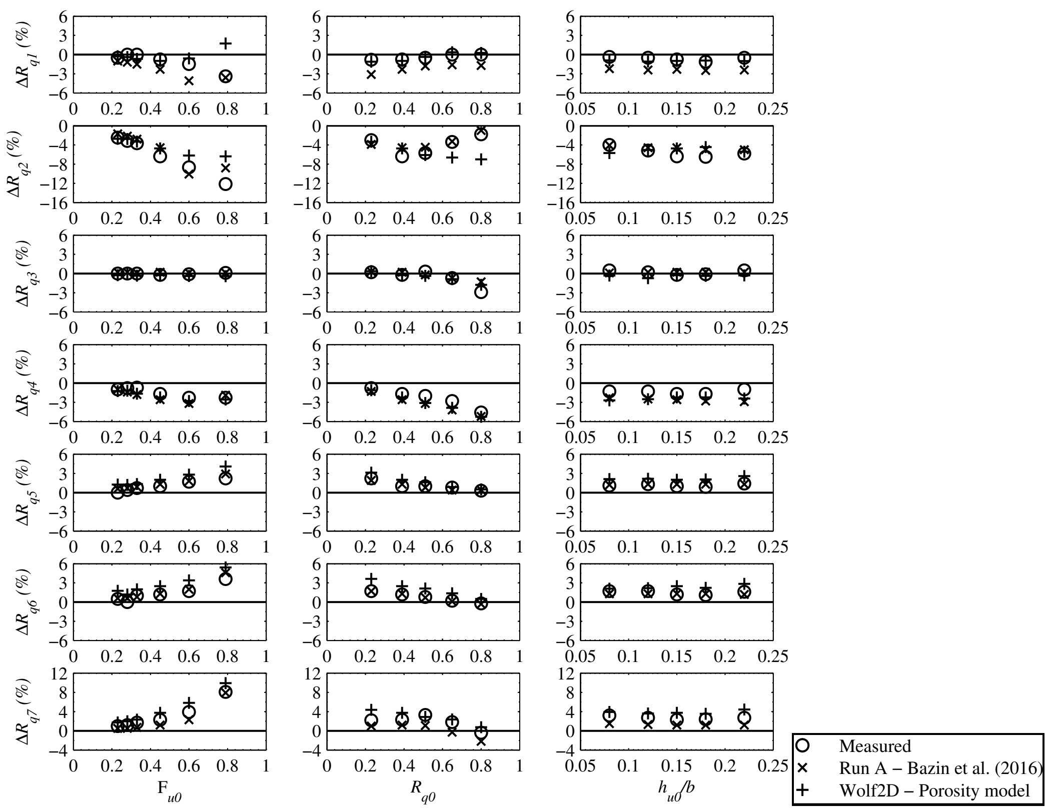

Figure 2 Change in the discharge partition due to the presence of the obstacle, as obtained from the experimental observations as well as from the numerical models of Bazin et al. (2016) and Arrault et al. (2016).

Table 1 Main characteristics and performance of the models used by the Authors and the Discussers for configurations without obstacles.

Numerical model	Computational mesh	Cell size	$\delta\left(Q_{b0}^{*}\right)$	$\sigma\left(Q_{b0}^{*}\right)$
Run A in Bazin et al. (2016)	Non-uniform	3.5-5 cm	-1.88%	2.50%
Arrault et al. (2016)	Coarse Cartesian grid	5 cm	-1.89%	3.56%

Table 2 Quality indicators obtained by authors and discussers for simulations with obstacles.

Numerical model	$\delta\left(\Delta R_{q1-7}\right)$	$\sigma\left(\Delta R_{q1-7}\right)$	$\delta\left(Q_{b1-7}^{*}\right)$	$\sigma\left(Q_{b1-7}^{*}\right)$
Run A in Bazin et al. (2016)	-0.37%	1.13%	-2.80%	3.79%
Arrault et al. (2016) - $c_D^0 = 2$	0.35%	1.25%	-0.65%	5.43%
Arrault et al. (2016) - $c_D^0 = 1$	0.32%	1.41%	-0.70%	5.94%
Arrault et al. (2016) - $c_D^0 = 3$	0.37%	1.4%	-0.61%	5.73%

Supplemental data

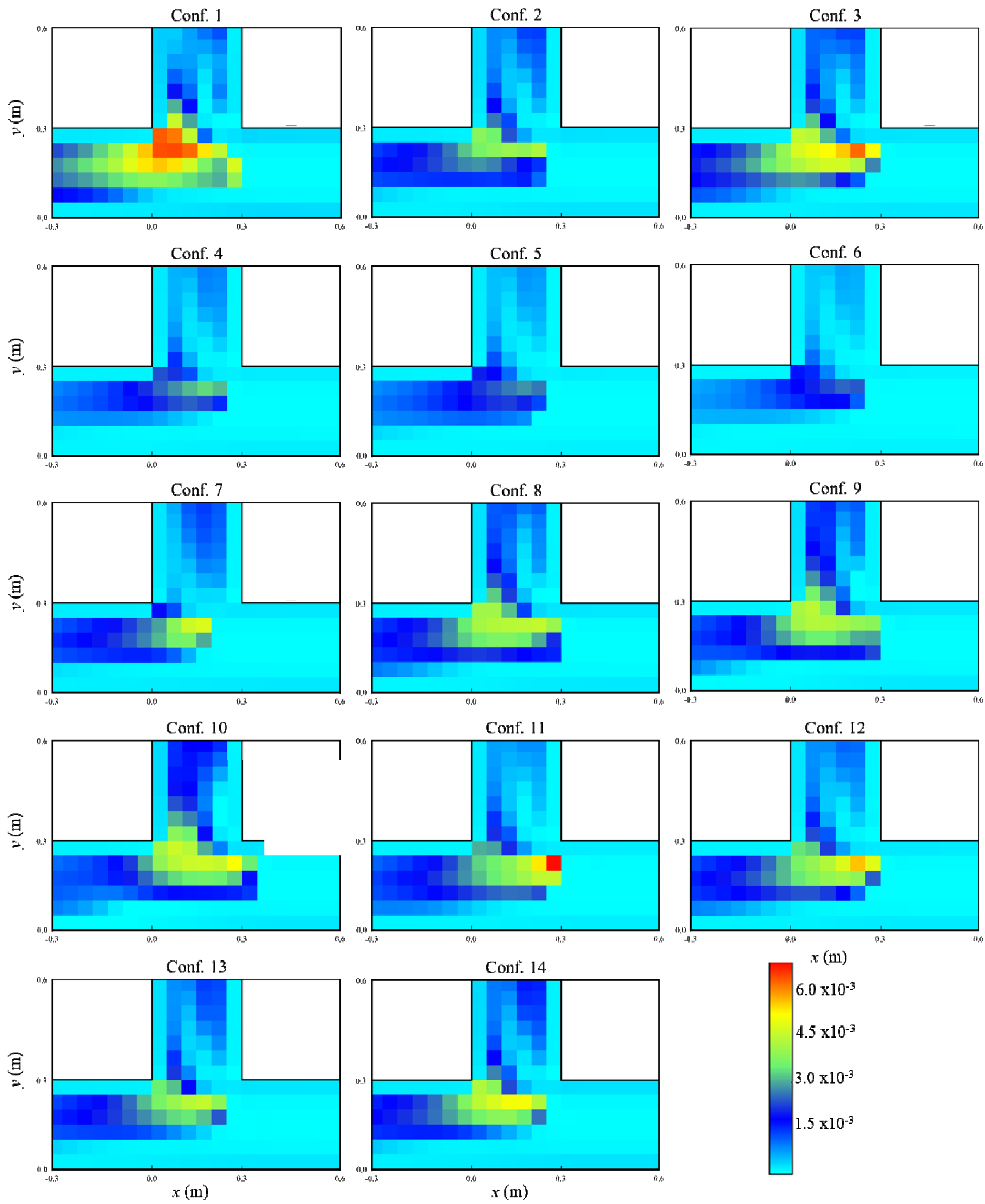

Figure S1: Computed maps of eddy viscosity for simulations without obstacles.

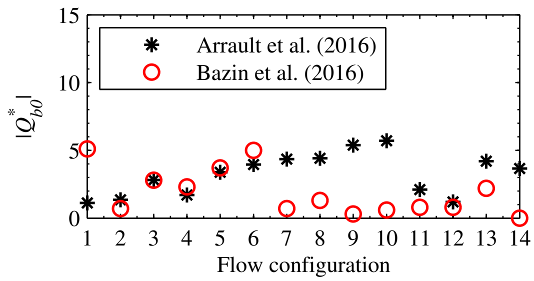

Figure S2: Absolute values of the relative errors of the lateral discharge Q^*_{b0} for simulations without obstacles.